SLAC–PUB–10327
January 2004

Simulation of electron cloud multipacting in solenoidal magnetic field*

A. Novokhatski and J.Seeman
Stanford Linear Accelerator Center, Stanford University, Stanford, California 94309

Abstract

A simulation algorithm is based on a numerical solution of the Vlasov equation for the distribution function of an electron cloud density in a cylindrical vacuum chamber with solenoidal magnetic field. The algorithm takes into consideration space charge effects. This approach improves the simulation of multipacting effects as it is free of statistical fluctuations. Simulation studies were carried for the SLAC B-factory vacuum chamber for different bunch patterns and solenoidal field strength. Space charge and the magnetic field limit the maximum density of the electron cloud. Magnetic resonant damping of multipacting was found in special cases of positron beam parameters and magnetic field amplitude.

Talk presented at the Seventh International Computational Accelerator Physics Conference

East Lansing, Michigan, USA

October 15-18 2002

* Work supported by Department of Energy contract DE–AC03–76SF00515.

Simulation of electron cloud multipacting in solenoidal magnetic field*

A. Novokhatski** and J.Seeman

Stanford Linear Accelerator Center, Stanford University, CA 94309

Abstract. A simulation algorithm is based on a numerical solution of the Vlasov equation for the distribution function of an electron cloud density in a cylindrical vacuum chamber with solenoidal magnetic field. The algorithm takes into consideration space charge effects. This approach improves the simulation of multipacting effects as it is free of statistical fluctuations. Simulation studies were carried for the SLAC B-factory vacuum chamber for different bunch patterns and solenoidal field strength. Space charge and the magnetic field limit the maximum density of the electron cloud. Magnetic resonant damping of multipacting was found in special cases of positron beam parameters and magnetic field amplitude.

1. Introduction

The electron cloud at PEP-II in the low-energy positron ring is built up from multipacting electrons in the straight section vacuum chamber and, perhaps, photo-emission and secondary emission of electrons from the vacuum antechamber in the arcs. Placing solenoidal magnetic fields around the ring successfully reduced multipacting and damped the electron cloud instability [1]. PEP-II has an upgrade plan that is leading toward higher luminosity by doubling the number of bunches and decreasing the spacing between bunches by a factor of 2 [2]. Here we describe the attempt to understand the possible effect from a new bunch pattern on electron cloud multipacting using the results of a computer simulation. We do not claim to make a universal simulation model for the electron cloud; we intend to study only the effect of solenoids on electron cloud multipacting in straight sections of PEP-II, as there were no such studies in previous works on tracking simulations [3-6] for PEP-II. KEK B factory has 3 times less bunch charge than PEP-II and multipacting effect may be less important. F. Zimmerman [7] calculated that only half of the electron cloud consists of secondary electrons in a solenoidal magnetic field of 50 Gauss. The first 3D simulation of the electron cloud in a magnetic field for the KEK B-factory [8] does not include secondary emission.

2. The model of electron cloud

The physical picture of the multipacting process leads us to use the phase distribution function for the best description of the electron cloud and for a precise modelling of secondary electron emission. It is worth noting that the usual approach of particle tracking can not accurately describe the secondary electron yield, because of statistical fluctuations: a large number of particles are needed in order to satisfy the wall boundary condition. The energy distribution of electrons which are emitted from a surface bombarded with primary electrons has a narrow peak of order 5 eV for "true'" secondary electrons, on the other hand, more over to have secondary emission yield more than one

* Work supported by US DOE contract DE-AC03-76SF00515

** novo@slac.stanford.edu

electron, the primary electrons must have tens or even hundreds of electron volts. This means the emitted electrons have to be accelerated by the field of positron bunches up to these energies in order to build up the multipacting process. In this way the initial angular distribution of emitted electrons does not play any considerable role, as the force vector from a positron bunch determines the vector of electron momentum. Without multipacting the number of primary electrons, coming from photoemission is not enough to create a considerable back action on the positrons.

In the straight sections of PEP-II the vacuum chamber is round and made from stainless steel. When a positron bunch is moving along the axis of a round tube it's electric field is radial and it also gives a radial kick to the cloud electrons. If the surface of the tube wall is azimuthally homogeneous (secondary emission yield is the same everywhere), then we can imagine that the electron cloud will also be azimuthally homogeneous. This means that we need only a two-dimension phase distribution function of radius and radial velocity for a complete description of the electron cloud in a straight section.

3. Vlasov equation and electromagnetic forces

The phase distribution function $\Psi(r,V)$ describes the density of the electron cloud on the phase plane of radius and radial momentum (velocity), as shown in Fig. 1.

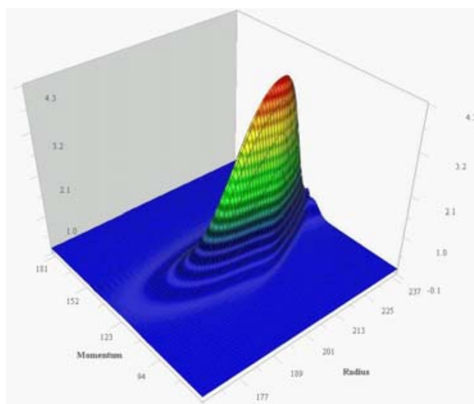

Figure 1: Phase distribution function on the phase plane of radius and radial momentum

This function obeys the Vlasov equation

$$\frac{\partial}{\partial t}\Psi + \frac{\partial}{\partial V}\Psi \times \frac{dV}{dt} + \frac{\partial}{\partial r}\Psi \times \frac{dr}{dt} = 0 \qquad \frac{dV}{dt} = \frac{F}{m_e} \qquad \frac{dr}{dt} = V$$

where F is the force acting on an electron from a positron bunch field, solenoidal magnetic field and electric field of other electrons (space charge force), m_e is the mass of an electron. Electric field of a positron bunch of the Gaussian shape is

$$E_{bunch}(r,t) = \frac{c}{2\pi r} \times \frac{Z_0 I^{+}_{bunch}}{f_{rev}} \times \frac{1}{\sigma\sqrt{2\pi}} \exp\left(-\frac{(ct)^2}{2\sigma^2}\right)$$

where I^{+}_{bunch} is the positron current per one bunch, σ is the positron bunch length, f_{rev} is the revolution frequency of particles in the positron ring and $Z_0 = 120\pi$ Ohm. The radial force from a solenoid is

$$F_{sol}/m_e = r*\Omega^2*\left(\left(\frac{a}{r}\right)^4*\left(1-\frac{\dot{\varphi}_0}{\Omega}\right)^2-1\right)$$

where a is the radius of the vacuum tube and $\Omega = \frac{e}{2mc}H$ is the Larmor frequency, $a\varphi_0$ is initial azimuthal velocity at the wall. Azimuthal motion is invariant

$$\mathrm{r}^2(\dot{\varphi}-\Omega) = const = a^2(\dot{\varphi}_0-\Omega)\,.$$

The space charge field has radial and longitudinal components (see Appendix). In the case of periodic series of positron bunches, when $E(t,z,r) = E(\tau,0,r)$ $\tau = t - z/c$ these components are:

$$E_r^{sc} = \frac{Z_0 c}{2}*e\bar{n}*\frac{a^2}{r}*\frac{\int_0^r (n+\frac{1}{Z_0 ec^2}\frac{\partial}{\partial\tau}E_z^{sc})r'dr'}{\int_0^a nrdr}$$

$$E_z^{sc}(r,\tau) = Z_0*\int_r^a j_r(r',\tau)dr'$$

where $\bar{n} = \frac{2}{a^2}\int_0^a nrdr$ is the space average electron cloud density and j_r is the radial electron cloud current.

Using these formulas it is very easy to estimate the acceleration (energy gain) of the cloud electrons from a kick of a positron bunch

$$W = \frac{m_e c^2}{2}*\left(\frac{Z_0 I_{bunch}^{+}}{m_e c f_{rev} 2\pi a}\right)^2$$

and the average electron cloud density

$$\bar{n}e = 2\frac{I_{bunch}^{+}}{\pi a^2 f_{rev}\lambda_{RF} N}$$

The spacing between positron bunches is equal to RF wavelength λ_{RF} multiplied by the spacing number N.

For typical PEP-II parameters:

$$I_{bunch}^{+} = 2mA,\ f_{rev} = 136kHz,\ a = 47.5mm,\ \lambda_{RF} = 63cm,\ N = 2$$

we have the following estimations:

$$W = 30.2\,eV \qquad \bar{n} = 2.06*10^{13}\ \ m^{-3}.$$

This means that an accelerated electron after returning back to the wall can produce more secondary particles (according to the secondary emission yield curve, presented in Fig.2). Saturated cloud density is of the order of the of residual gas density in the vacuum chamber ($p \sim 10^{-9}$ Torr).

4. Computer algorithm

A double-step semi-implicit finite-difference scheme with a diffusion parameter α is to model a numerical solution of the Vlasov equation

$$22\Psi_{i,k}^{n+1}+\Psi_{i,k+1}^{n+1}+\Psi_{i,k-1}^{n+1}=22\Psi_{i,k}^{n}+\Psi_{i,k+1}^{n}+\Psi_{i,k-1}^{n}-24\frac{\Delta t}{\Delta r}V_j\left(\Psi_{i,k+1/2}^{n+1/2}-\Psi_{i,k-1/2}^{n+1/2}\right)$$

$$a\Psi_{i,k}^{n+1}+\Psi_{i+1,k}^{n+1}+\Psi_{i-1,k}^{n+1}=b\Psi_{i,k}^{n}+c(\Psi_{i+1,k}^{n}+\Psi_{i-1,k}^{n})-d\frac{\Delta t}{\Delta V}F_k\left(\Psi_{i+1/2,k}^{n+1/2}-\Psi_{i-1/2,k}^{n+1/2}\right)$$

$$a=\frac{22+2\alpha}{1-\alpha}\quad b=\frac{22-2\alpha}{1-\alpha}\quad c=\frac{1+\alpha}{1-\alpha}\quad d=\frac{24}{1-\alpha}$$

This scheme has a very good dispersion relation

$$\sin\frac{\omega\Delta t}{2}=\frac{12}{11}V\frac{\Delta t}{\Delta r}\frac{\sin\frac{k\Delta r}{2}}{1+\frac{1}{11}\cos(k\Delta r)}$$

Wave vector is linear with frequency $\omega\cong Vk$ in the region up to half the mesh-size frequency. Small value of the diffusion parameter $\alpha=0.005$ being needed to compensate oscillations at the mesh-size frequency.

Boundary conditions are described by secondary electron emission probability functions $P(\varepsilon_{in},\varepsilon_{out})$

$$\Psi_{in}(r=a)*V_{in}=\Psi_{out}(r=a)*V_{out}\times P\,(\varepsilon_{in},\varepsilon_{out})$$

The probability function is a combination of secondary emission yield and a spectrum of secondary electrons. Experimental data is used for this function specification.

The code was written in Fortran 90 using graphical library “Array Viewer”. A typical number of mesh points is 500*500. Typical computer time (1GHz PC) for a 1μsec multipacting process is about 12 hours. The code is not yet completely optimized.

5. Secondary emission functions

Secondary emission yield for stainless steel, as a function of the energy of the primary electron is presented in Fig2

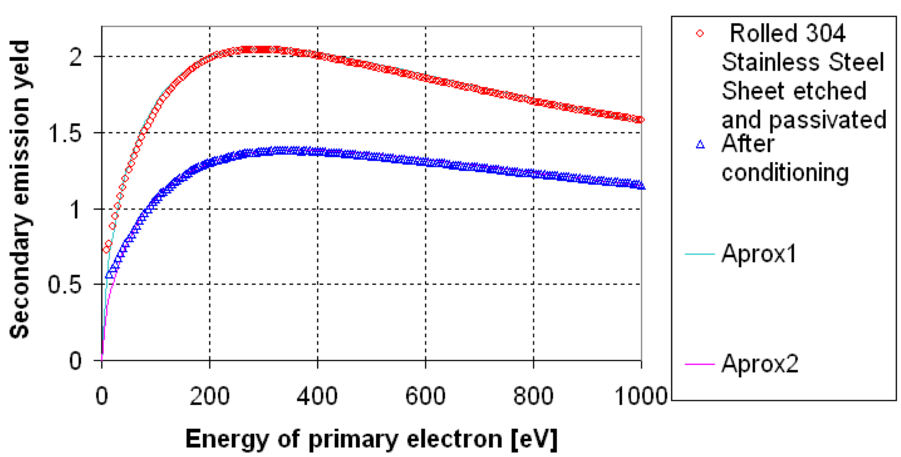

Figure 2: Secondary electron emission yield**.**

The measurements were done at SLAC by R.E. Kirby [9-11]. The smaller yield curve shows the reduction of the secondary emission yield with conditioning. We can suggest that the real yield is somewhere between this curves, however in simulations we take the worst case. Approximation curves used in simulations are also shown. We extrapolate to zero yields for zero energy of the primary electrons. The energy spectrum of the secondary electrons includes inelastically backscattered and elastically reflected electrons [11]. We use R.E. Kirby results of the spectrum measurement for two primary electron energies (Fig.3) to extrapolate spectrums to other energies.

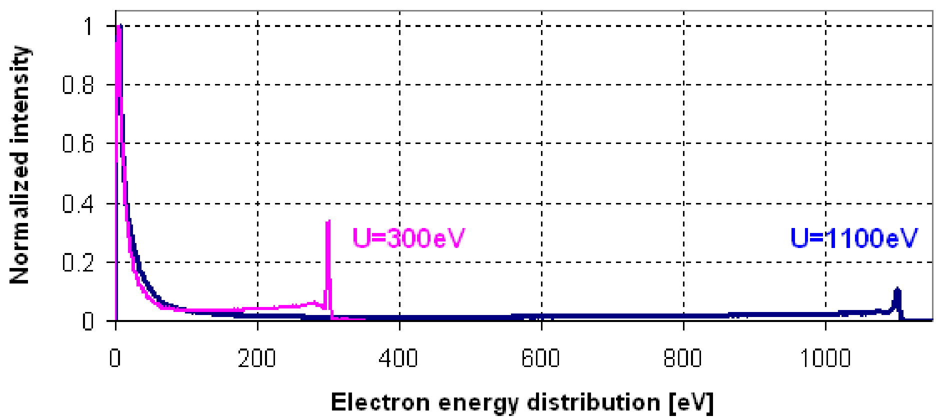

Figure 3: Normalized spectrum of secondary electrons for normal incident primary electrons of 300eV and 1100eV from clean stainless steel.

6. Multipacting at small solenoidal fields

First simulations were carried for small values of a solenoidal field to study the growth rates of cloud density due to multipacting. We start with some initial distribution of electrons then let positron bunches appear periodically in time and watch how the electron cloud density changes in time. Fig.4 shows the dynamics of cloud density with a positron train of a bunch spacing by 2 and bunch current of 2mA for different values of solenoidal field. Logarithm functions of density are shown on the right side together with linear approximations. At the beginning, the density increases exponentially, but saturates due to the action of space charge forces. Higher solenoidal fields not only decrease the growth rate, but also change the growth function from pure exponential to a square root dependence of time.

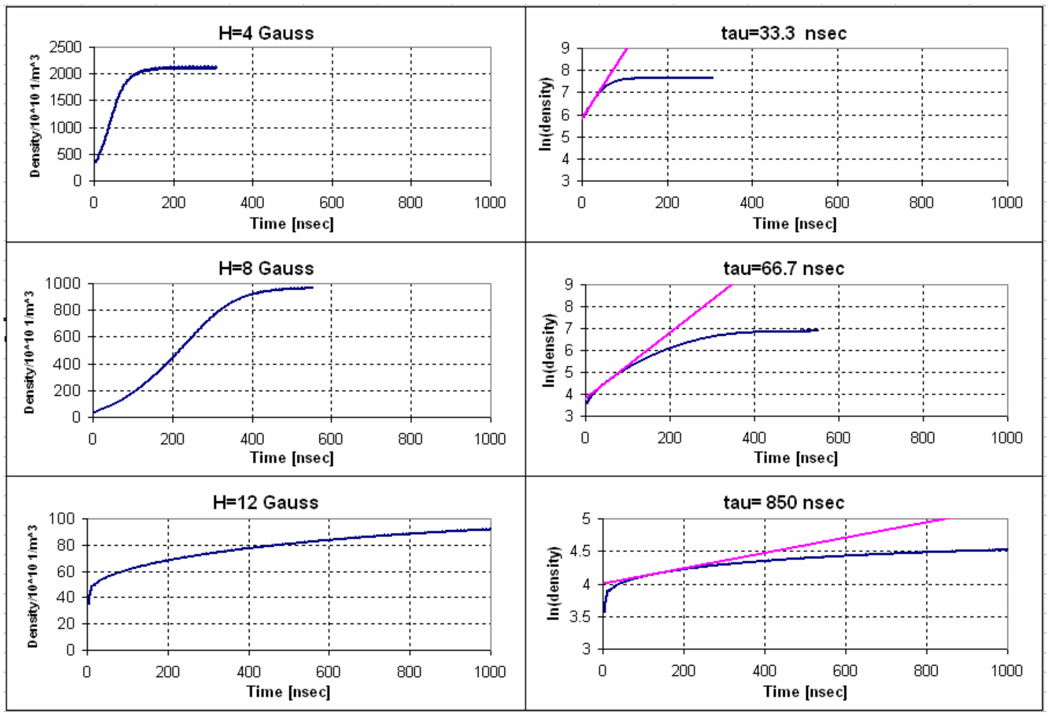

Figure 4 Dynamics of electron cloud density for different values of solenoidal field. Logarithm functions of density are shown on the right side.

Electron cloud distribution on the phase plane (image plot) is shown on Fig.5. Particles travel from chamber axis to the wall in the upper half part of the plot and from the wall to the axis in the lower half part. In the phase plot, radial momentum is measured in equivalent of electron volts. The radial distribution is shown in the right part of Fig.5. The picture shows the cloud at the moment between two positron bunches. Solenoidal magnetic field is 8G. It is possible to see that the cloud comprises five secondary bunches.

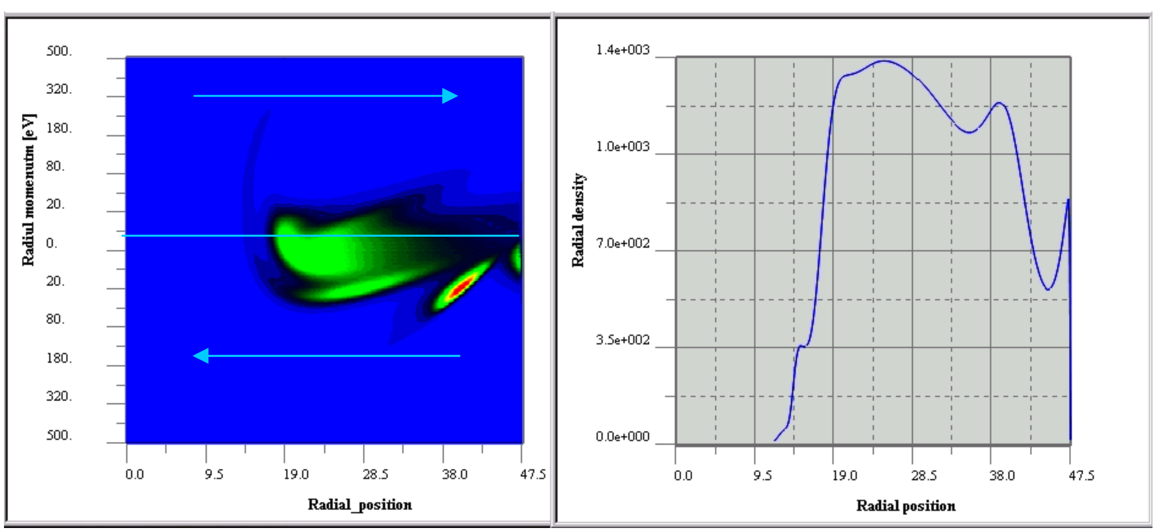

Figure 5: Electron cloud on the phase plane. Light blue line depicts zero velocity line. Arrows show the directions of particle motions. Radial cloud distribution is on the right.

7. Main resonance

While studying the behaviour of the electron cloud for different solenoidal fields we found a strong resonance. This resonance happens when the time interval between the positron bunches is equal to the flight time of the secondary particles back to wall. The flight time is mainly determined by the solenoidal field H and partially by the cloud size and intensity. Naturally the resonance depends strongly upon the secondary emission function. The resonance is the boundary between completely different behaviours of the electron cloud. Multipacting happens when the flight time is a little bit smaller than the positron time interval; when the solenoidal field is a little bit higher than the resonance field $H > H_{res}$. And there is no multipacting if $H < H_{res}$. Fig.6 demonstrates this effect. A difference of the solenoidal field of only 1 Gauss completely changes the behaviour of the cloud.

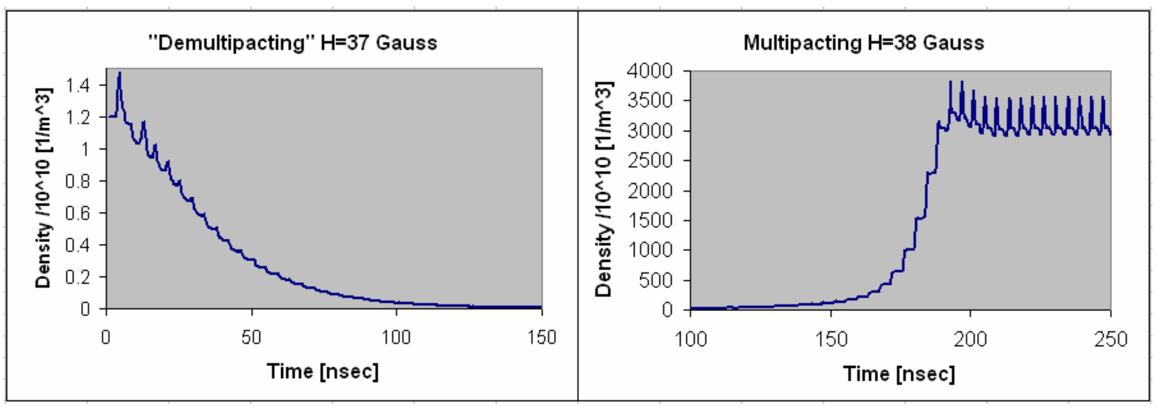

Figure 6: Cloud density behaviour in the resonance region.

Corresponding phase photos (high plots) of the clouds are shown at Fig.7. Clouds are "shot" just before positron bunch arrives.

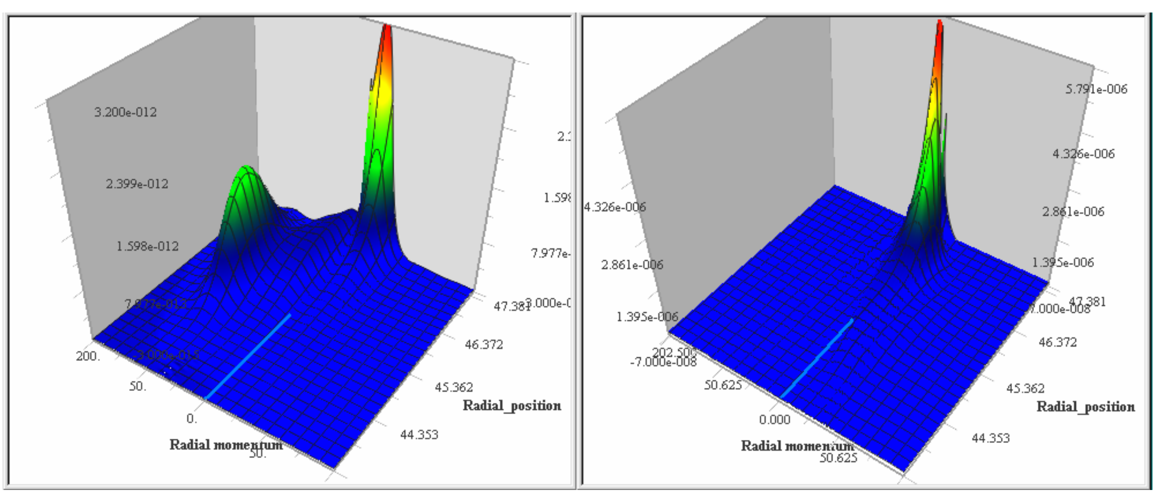

Figure 7: Electron clouds on the phase plane just before a positron bunch arrives. The left picture is for a solenoidal filed H= 37G and the right picture for H=38G. The light blue lines depict the zero velocity line.

Secondary particles, previously produced by high-energy particles are ready to be accelerated by the next positron bunch. After acceleration they will come back to the wall and produce more new particles. It is possible to see that "right" cloud mainly consists of secondary particles. However "left" cloud has additional high-energy peak, which will be decelerated by positron bunch and will arrive at the wall with very little energy and hence will not produce new secondary particles. Therefore the density will go down and finally "left" cloud will waste away.

8. Other resonances

We can assume that there can be some other resonances. A resonance can also happen if the flight time of the secondary particle is equal to an integer number of time intervals between positron bunches.

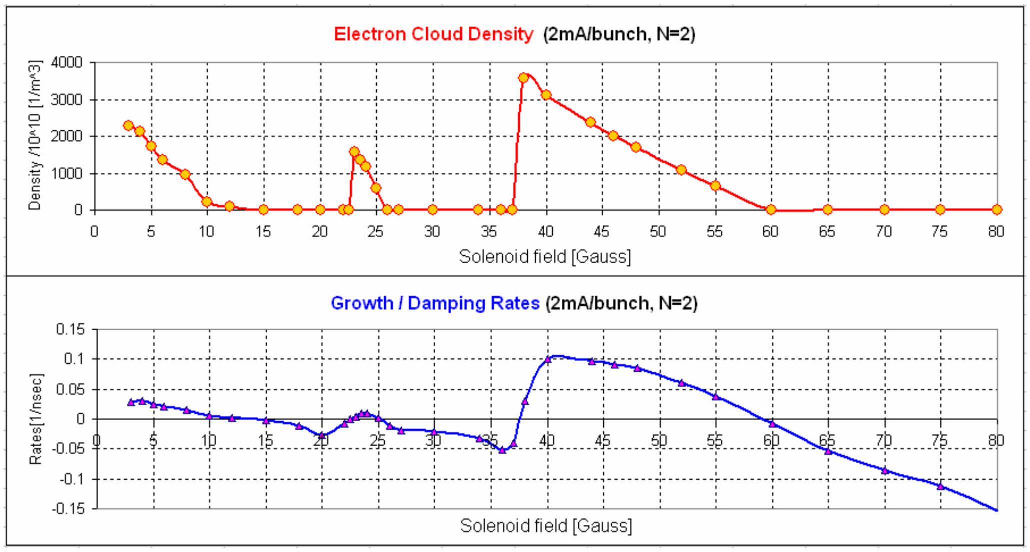

Figure 8: Electron cloud saturated density and growth/damping rates as a function of the solenoidal field for a positron train with a bunch spacing by 2.

These resonances happen at smaller values of solenoidal field. In our case we have a second resonance at the solenoidal field of 23G. Other resonances are in the region below 10 G. Fig.8 shows the saturated values of the electron cloud as a function of the solenoidal field and growth/damping rates. Negative values mean that the cloud wastes away after some time. There is no multipacting when solenoidal field is more than 60 G. Clear regions are also in the gap of 26-36 G and 14-22 G.

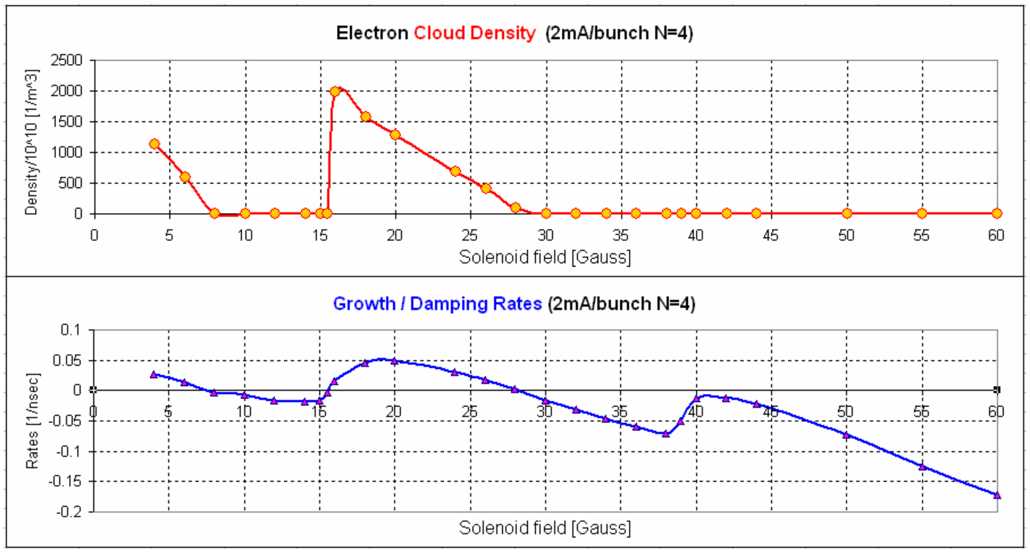

Figure 9: Electron cloud saturated density and growth/damping rates for a positron train with bunch spacing by 4.

For comparison with Fig.9 we present analogue curves for the electron clouds with a positron train with spacing by 4. The main resonance is moved to 16 G, other resonances are in the region below 8 G. No multipacting after 30 G and in the gap 8-15 G. It is interesting to note that in the region of 39 G there is a jump in the damping rate. It is possible to suggest that it is a half integer resonance: the forced frequency from the field of positron bunches is two times smaller than the repetition rate of the secondary electron emission.

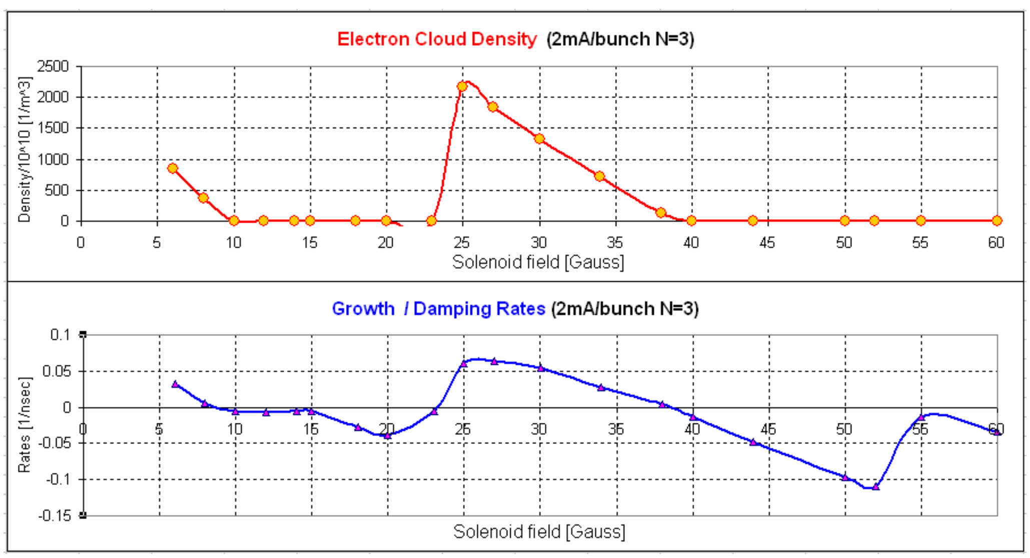

Figure 10: Electron cloud saturated density and growth/damping rates for a positron train with bunch spacing by 3.

In the intermediate case when the positron bunch train has a spacing of 3 RF buckets the resonance value for solenoidal field is 25 G and zones with no multipacting are after 40 G and between 10-24 G. Half integer resonance is in the region of 53 G (Fig.10).

9. Longitudinal electron cloud field

In order to build electron cloud, positron bunches have to use some amount of their kinetic energy. The field, which is responsible for the energy transformation, is longitudinal electric field. When the cloud is already built, this longitudinal field acts as an oscillating force on the cloud electrons and gives, at the same time, an additional energy variation inside the positron bunches. The head of the positron bunch is accelerated and the tail is decelerated. This action of the longitudinal field is similar to the action of RF fields in a cavity. As a result the positron bunches will have different lengths throughout the train. This effect can be checked in experiment. Fig. 11 shows a longitudinal field together with the positron bunch shape. The solenoidal field is 38G, bunch spacing is two RF buckets. The energy variation along a positron bunch is more than 100 V on 1 m of vacuum chamber. The total length of all straight sections in the positron storage ring is around 740 m, so the total effect of the electron cloud can be of order of 74 kV, which is equivalent to 185 kV of RF voltage at 476 MHz. It is easy to make an analytical estimation for this effect. The additional variation of energy in a positron bunch for one meter of vacuum chamber due to the electron cloud is

$$\Delta W / l = \frac{2}{\lambda_{RF} * \mathrm{N}} m_e c^2 * \left(\frac{Z_0 I^{+}_{bunch}}{m_e c f_{rev} 2\pi a} \right)^2$$

This formula gives the same result, as we got from the computer simulations.
The longitudinal effect on the positron bunches might be very important. In previous papers [12-13] longitudinal effects were discussed but only with respect to motion of the electrons in the cloud.

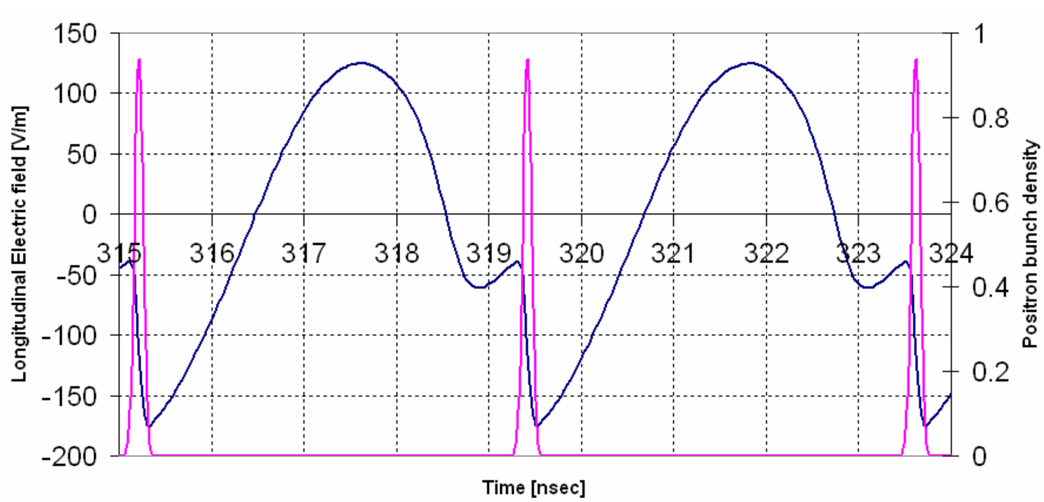

Figure 11: Longitudinal electric field in electron cloud. Solenoidal field is 38 G, bunch spacing is two RF buckets.

10. Conclusions

Computer simulations show that increasing the number of positron bunches by a factor of two and keeping the same current per bunch means that the solenoidal field needs to be doubled in order to keep the same electron cloud density. Currently PEP-II solenoids in straight sections have nearby 30 gauss [1], so we need to increase the field up to 60 gauss. Fortunately there are regions that are "free of multipacting" at smaller values of solenoidal field where the electron cloud density can not get very high. This prediction of low cloud density can be checked in experiment.

Acknowledgement

The authors thank R.E. Kirby for important information about secondary emission process and presented files of SEY measurements. We thank A. Kulikov who first pointed out this problem and M. Sullivan for fruitful discussions and very useful remarks.

Appendix

The formulas for the space charge electric field components of an azimuthally symmetric and longitudinally periodic electron cloud, are derived from the Maxwell equations

$$div\varepsilon_0\vec{E} = en \quad rot\vec{H} = \frac{\partial}{\partial t}\varepsilon_0\vec{E} + \vec{j} \quad rot\vec{E} = -\frac{\partial}{\partial t}\mu_0\vec{H}$$

The equations for azimuthally symmetrical fields in a cylindrical coordinate system are

$$\frac{1}{r}\frac{\partial}{\partial r}rE_r + \frac{\partial}{\partial z}E_z = en/\varepsilon_0 \quad -\frac{\partial}{\partial z}H_\varphi = \varepsilon_0\frac{\partial}{\partial t}E_r + j_r \quad \frac{\partial}{\partial z}E_r - \frac{\partial}{\partial r}E_z = -\mu_0\frac{\partial}{\partial t}H_\varphi$$

Now we use the assumption that electron cloud has a periodic structure

$$E(t,z,r) = E(\tau,0,r) \quad \tau = t - z/c$$

$$\frac{\partial}{\partial z}E_{r,z} = -\frac{1}{c}\frac{\partial}{\partial \tau}E_{r,z} \quad \frac{\partial}{\partial z}H_\varphi = -\frac{1}{c}\frac{\partial}{\partial \tau}H_\varphi$$

This assumption works well for the case when you have a periodic positron bunch pattern (what we have in mini trains in PEP-II) and relatively long vacuum chambers with solenoids. In the PEP-II straight sections we have solenoids of approximately 6 m long and a distance between positron bunches at 2.5 m (bunch pattern by 4) or 1.25m (bunch pattern by 2).

Together with the relation

$$\varepsilon_0 = \sqrt{\frac{\varepsilon_0}{\mu_0}}\sqrt{\varepsilon_0\mu_0} = \frac{1}{Z_0 c}$$

we have

$$\frac{1}{r}\frac{\partial}{\partial r}rE_r = enZ_0c + \frac{\partial}{c\partial \tau}E_z \quad \frac{1}{c}\frac{\partial}{\partial \tau}(H_\varphi - \frac{1}{Z_0}E_r) = j_r \quad \frac{\partial}{\partial r}E_z = \frac{1}{c}\frac{\partial}{\partial \tau}(Z_0H_\varphi - E_r) = Z_0 j_r$$

Integration in the radial direction and using the boundary condition $E_z(r = a,\tau) = 0$ finally gives the following equations

$$E_r = \frac{1}{r}\int_0^r (eZ_0cn + \frac{\partial}{c\partial \tau}E_z)r'dr' \quad E_z(r,\tau) = Z_0 * \int_r^a j_r(r',\tau)dr'$$

For convenience we rewrite the first part in the following form

$$E_r = \frac{Z_0 c}{2} * e\overline{n} * \frac{a^2}{r} * \frac{\int_0^r (n + \frac{1}{Z_0 e c^2} \frac{\partial}{\partial \tau} E_z) r' dr'}{\int_0^a nrdr} \qquad \overline{n} = \frac{2}{a^2} \int_0^a nrdr$$

References

[1] A. Kulikov, A. Fisher, S. Heifets, J. Seeman, M. Sullivan, U. Wienands, W. Kozanecki, “The Electron Cloud Instability at PEP-II B-Factory”, PAC’2001, Chicago, June 2001, p. 1903

[2] J.Seeman et al., “PEP-II Status and Future Plans”, EPAC 2002, Paris, June 2002, p. 434.

[3] M. A. Furman and G. R. Lambertson, “The Electron-Cloud Instability in the Arcs of the PEP-II Positron Ring”, LBNL-41123/CBP Note-246, PEP-II AP Note, AP 97.27, November 25, 1997.

[4] M.A. Furman and G.R. Lambertson, “The Electron-Cloud Instability in PEP-II: An Update”, Proc. of 1997 PAC, Vancouver (May 1997) (pub 1998) p. 1617.

[5] A. Chao and M.Tigner “Handbook of Accelerator Physics and Engineering”, World Scientific, 1998, p.131-133.

[6] Y. Cai, S. Heifets, J. Seeman, M. Furman, M. Pivi, “New Simulation Results for the Electron-Cloud Effect at the PEP-II Positron Ring”, Proc. of 2001 PAC, Chicago (Jun. 2001) p. 698.

[7] F. Zimmerman “Electron Cloud at the KEK Low-Energy Ring: Simulation of central Cloud Density, Bunch Filling Patterns, Magnetic Fields, and Lost Electrons”, CERN-=SL-2000-017(AP), June 2000.

[8] L. Wang, H. Fukuma, K. Ohmi, “3D Simulation of Photoelectron Cloud Instability”, Proc. of 2001 PAC, Chicago (Jun. 2001), p.702

[9] R. Kirby, Private communication

[10] R.E. Kirby and F.K. King, “Secondary electron emission yield from PEP-II accelerator materials”, NIM A 469(2001) p.1

[11] P.A. Redhead, J.P. Hobson, E.V. Kornelsen, “The Physical Basis of Ultrahigh Vacuum”, AIP, New York, 1993, p134.

[12] G. Rumolo, F. Zimmermann, 'Longitudinal Field due to Electron Cloud', Proc. KEK Two-Stream Instabilities Workshop, KEK, September 2001, and in CERN-SL-2001-067 (AP)

[13] T. Katsouleas, A. Ghalam, S. Lee, W. More, C. Huang, V. Decyk, C. Ren, ``Plasma Modelling of Wakefields in Electron Clouds," Proc. ECLOUD'02 Workshop, CERN, Geneva, April 2002, CERN-2002-001.